

Stability analysis on the concrete slab of the highest concrete-faced rock-fill dam in South Korea

Seung-Hyung Baak¹, Gye-Chun Cho^{*1} and Ki-II Song²

¹*Department of Civil and Environmental Engineering, Korea Advanced Institute of Science and Technology, Daejeon, 34141, Republic of Korea*

²*Department of Civil Engineering, Inha University, Incheon, 22212, Republic of Korea*

(Received May 27, 2015, Revised July 20, 2017, Accepted July 8, 2017)

Abstract. Design and management of concrete slabs in concrete-faced rock-fill dams are crucial issues for stability and overall dam safety since cracks in the concrete face induced by stress, shrinkage, and deterioration can cause severe leakage from the reservoir into the dam. Especially, the increase of dam height to a certain level to enhance the storage capacity and to improve hydraulic stability can lead to undesirable deformation behavior and stress distribution in the existing dam body and in the concrete slabs. In such conditions, simulation of a concrete slab with a numerical method should involve the use of an interface element because the behavior of the concrete slab does not follow the behavior of the dam body when the dam body settles due to the increase of dam height. However, the interfacial properties between the dam body and the concrete slab have yet to be clearly defined. In this study, construction sequence of a 125 m high CFRD in South Korea is simulated with commercial FDM software. The proper interfacial properties of the concrete slab are estimated based on a comparison to monitored vertical displacement history obtained from the concrete slab. Possibility of shear strength failure under the critical condition is investigated based on the simplified model. Results present the significance of the interfacial properties of the concrete slab.

Keywords: CFRD; concrete slab; back analysis; interface element; numerical analysis

1. Introduction

Design and management of concrete slabs in concrete-faced rock-fill dams are crucial issues for the stability and overall dam safety since cracks in the concrete face induced by stress, shrinkage, and deterioration can cause severe leakage from the reservoir into the dam. Once a slab has fissures, it can be easily shattered due to hydraulic pressure in the critical level of reservoir. So, this can easily lead to stability problems. Especially, the increase of dam height to a certain level to enhance the storage capacity and to improve hydraulic stability can lead to undesirable deformation behavior and stress distribution in the existing dam body and in the concrete slab. In such conditions, simulation of the concrete slab with numerical method should involve the use of an interface element because the behavior of the concrete slab does not follow the behavior of the

*Corresponding author, Professor, E-mail: gyechun@kaist.edu

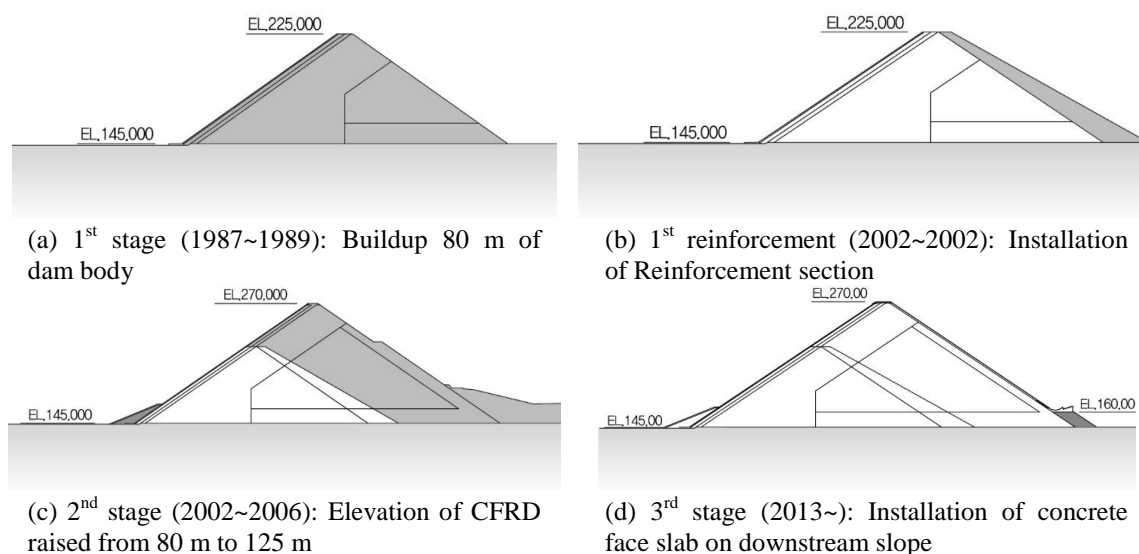


Fig. 1 Construction stage of the highest CFRD in South Korea

dam body when the dam body settles due to the increase of dam height.

The target of this study is the stability of a concrete slab of the highest CFRD under construction in South Korea. As it can be seen in Fig. 1(a), the 1st stage of an 80 m high CFRD was constructed from 1987 to 1989. The upstream slope was covered with a 0.8 m thick concrete slab in this stage. In 1995, the capacity of the CFRD was re-focused because of localized heavy rainfall in the northern part of the CFRD basin. Thus, supplementary reinforcement for the 1st construction was performed in 2002, as shown in Fig. 1(b), to increase the height of the CFRD. In 2006, the elevation of the CFRD and the concrete slab finally reached 125 m after the 2nd construction stage. Currently, reinforcement work (3rd stage) is proceeding to increase the stability of the CFRD against overflow. In the 3rd stage construction, a 1 m thick concrete face will be installed over the downstream slope.

Raising the height of a CFRD usually leads to deformation of the dam body because rock-fill acts as a load (Shin 2007). Thus, it is obvious that upstream concrete slabs will be affected by any subsequent construction process. However, study of the stability of concrete slabs due to sequential construction has been insufficient. Thus, in this study, the construction sequence of a 125 m high CFRD in South Korea is simulated using a numerical method. Proper interfacial properties of concrete slabs are estimated based on the vertical displacement history obtained on the concrete slabs. Possibility of shear strength failure under the critical condition is investigated.

2. Back analysis of CFRD

2.1 Monitoring of the vertical settlement

Fig. 2 shows the vertical deformation and vertical strain obtained at the crest of the CFRD since 1992. It can be seen that settlement and strain have linearly increased since 2006. The tracing of a triangle in Fig. 2(a), which indicates the vertical displacement after the 2nd construction stage, is

steeper than the tracing of the square, which indicates the vertical displacement after the 1st construction stage. Interestingly, the vertical strain, obtained after the 2nd construction stage, shows a value similar to that obtained during the 1st construction stage. This is because the elevation was increased from 80 m to 125 m.

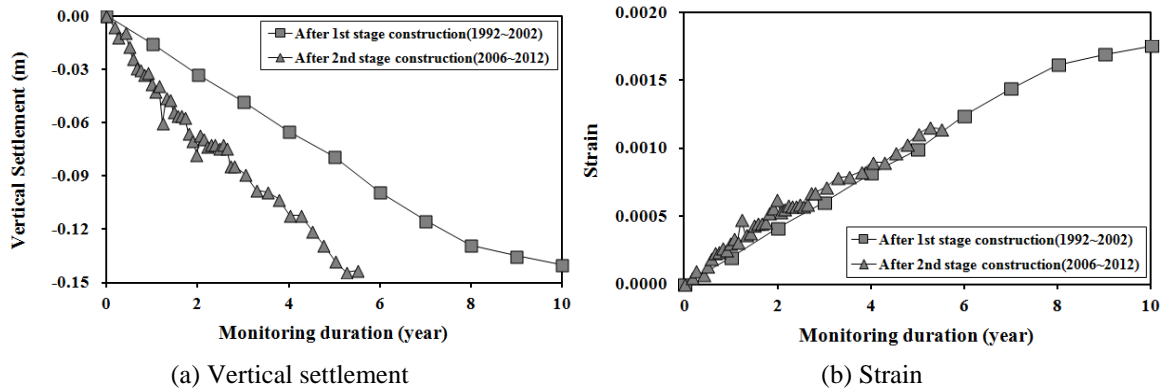


Fig. 2 Vertical settlement and strain history at CFRD crest

Table 1 Kelvin model

Type	Visco-elastic model	Stress-strain curve
Kelvin		

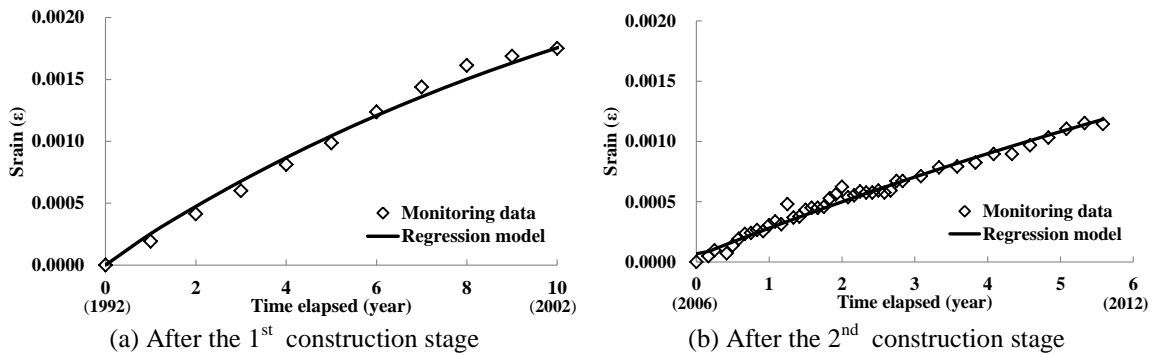


Fig. 3 Regression analysis with least square solution

Table 2 Kelvin model parameters obtained from the least square regression

Stage	Average $\Delta\sigma_1$ (kN/m ²)	K_K (kN/m ²)	G_K (kN/m ²)	η_K
After 1 st stage	241	5.29E7	1.40E4	5.50E7
After 2 nd stage	390	1.11E6	2.10E4	9.41E7

2.2 Time-dependent behavior of CFRD

Based on the monitoring data, the crest of the CFRD can be said to show time-dependent behavior. Regularly, the long-term behavior of the CFRD can be presented as either elastic or visco-elastic. The soil, which also shows time-dependent behavior, can be modeled by combining the elastic model and the visco-elastic model. Elastic behavior can be simulated with spring and viscostic behavior can be modeled with dashpot. Kelvin suggested a model that can express visco-elastic behavior by combining a spring and dashpot, as presented in Table 1 (Yoon and Song 2016).

In this study, the Kelvin model is adopted to predict the long-term settlement behavior of CFRD. The governing equation of the Kelvin model in the triaxial compression state can be expressed as in Eq. (1)

$$\epsilon(t) = \frac{1}{9K_k} (1 + 2K_0)\Delta\sigma_1 + \frac{1}{3G_k} (1 - 2K_0)\Delta\sigma_1 [1 - e^{-(G_k t / \eta_k)}] \tag{1}$$

where K_k , G_k , and η_k are the Kelvin model parameters and $\Delta\sigma_1$ and K_0 are the increment of maximum principal stress and the earth pressure coefficient at rest, respectively. To obtain the Kelvin model parameters, least square regression is carried out with the monitoring data by using MathCad as presented in Fig. 3. Procedure to determine the Kelvin model parameters of dam body depending on the construction stage is presented in Mathgram 1. Kelvin model parameters after the 1st construction stage and the 2nd construction stage are summarized in Table 2.

2.3 Prediction of long-term behavior of CFRD with Kelvin model

The long-term strain curves after each construction stage are presented in Fig. 4 with regressed Kelvin models. After the 1st construction stage, the dam strain ($\epsilon_{(t=2002)}$) in 2002 was estimated at 0.00175. Strain ($\epsilon_{(t=\infty)}$) for the 1st body is predicted to converge to 0.002872. However, this stage was not reached due to the confining stress induced by the 2nd construction stage. After the 2nd construction stage in 2006, the strain ($\epsilon_{(t=2013)}$) in 2013 was estimated at 0.001386, at which point the 3rd construction stage started and the strain was expected to converge to 0.003176 ($\epsilon_{(t=\infty)}$). The strain level, estimated with the Kelvin model at convergence ($\epsilon_{(t=\infty)}=0.31\%$), satisfies the local guideline that maximum strain of a dam should be within the range of 0.1-0.35%, according to the ‘‘Guidelines for design of dams’’ (Ministry of Land, Infrastructure and Transport 2011).

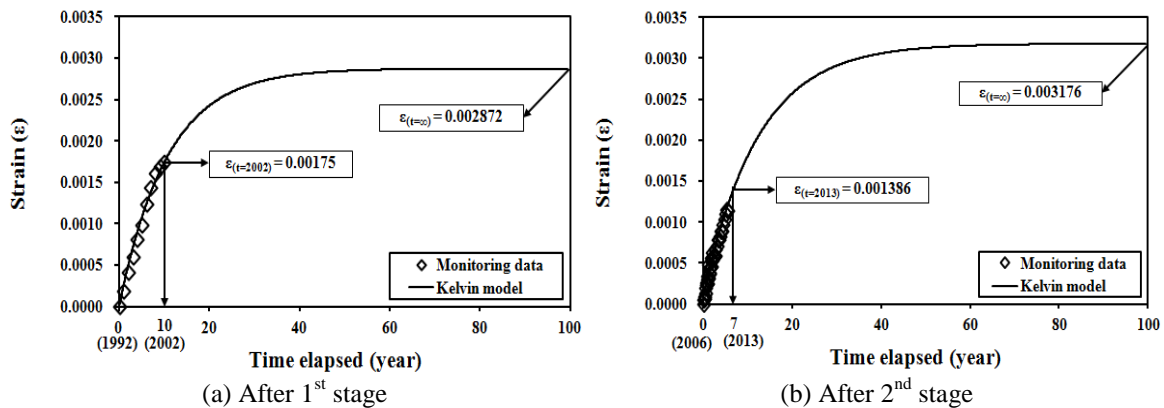


Fig. 4 Prediction of long-term behavior with Kelvin model

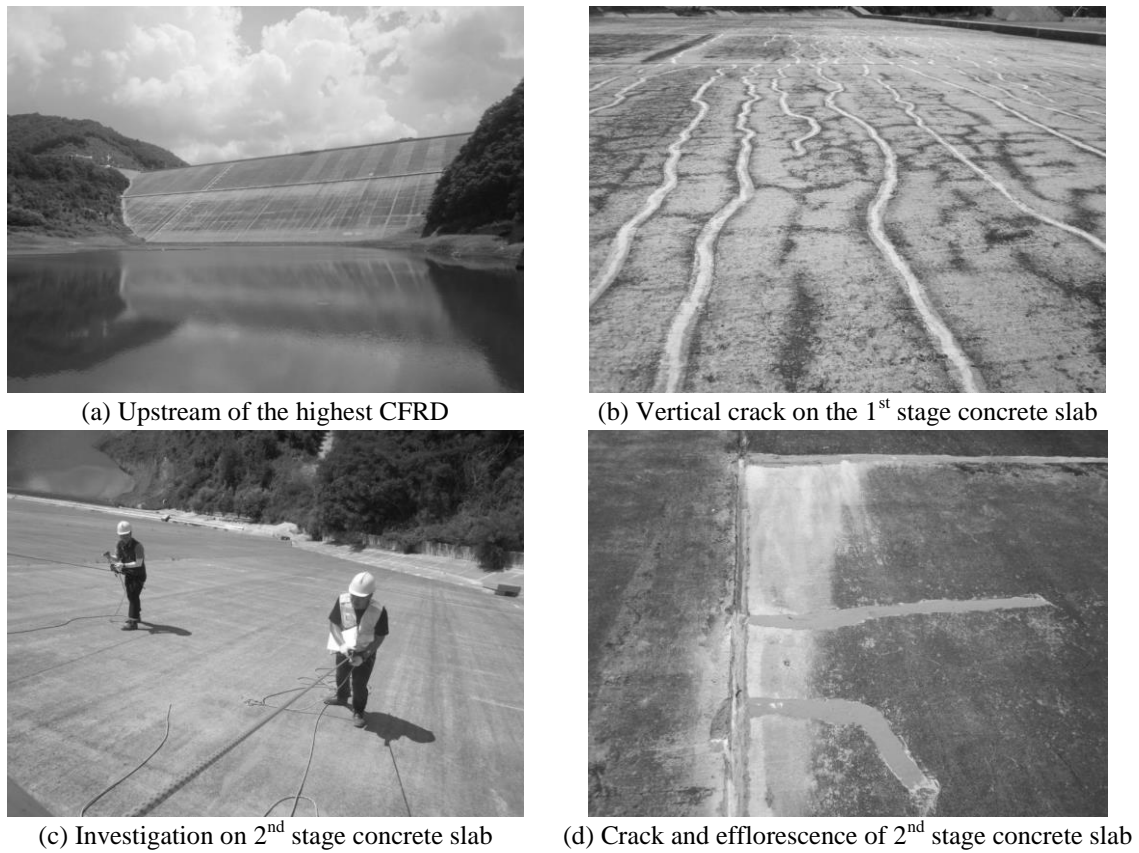


Fig. 5 Investigation and result on the concrete slab at the highest CFRD in Korea

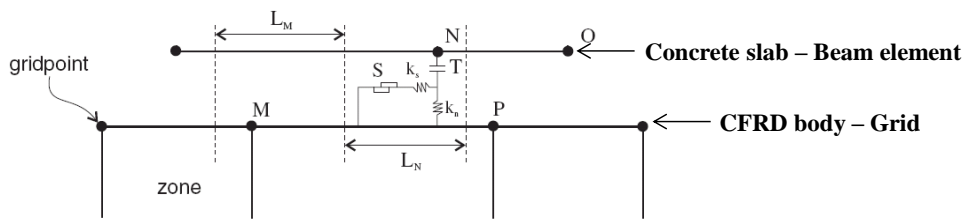


Fig. 6 Modeling of interface element in FLAC2D

3. Stability analysis on concrete slab

3.1 Problems related to concrete slab

In CFRD, the quality of concrete slab is the most important issue. Crack of concrete slab is associated to stability problem. Failure of CFRD can be induced due to seeping through the crack on the concrete slab. Crack can be generated due to construction joint, bending behavior due to external force, shrinkage during curing process and compressive and shear force. Moreover, creep behavior of CFRD is the crucial factor that causes crack.

The target CFRD studied is the highest CFRD in Korea. Considering the specification of slip form, winch, mobility of concrete and expansion of concrete, span of each concrete slab is determined as 15 m and the 0.3 m thick concrete slab is selected for second construction stage to make the concrete slab continuous. Therefore, there should be vertical construction joints between concrete slabs only. The ratio of steel to concrete is 0.4%. Steel reinforcement is enhanced for outer slab and perimetric joint where the tensile force is critical.

Fig. 5(a) shows the upstream view of the highest CFRD in Korea. The concrete slab constructed in the first stage contains vertical cracks and horizontal crack at the upper part of the 1st stage concrete slab. Micro-cracks (less than 0.2 mm), efflorescence, crazing, failure of sealing material and vegetation in the crack are the problems found in the 1st stage and the 2nd stage concrete slabs in this CFRD from site investigation.

Aforementioned problems related to concrete slab are essential for this CFRD. To secure the long-term stability of CFRD, it is necessary to find the causes of crack and introduce the best measures. Moreover, to secure the stability of this CFRD during the overflow condition and against seismic loading, reliable analysis on the CFRD and maintenance of the concrete slab should be performed regularly.

3.2 Use of interface element

Generally, concrete slabs in CFRDs are installed on the top of the slope, with minimum adhesion. Adhesion between the concrete slab and the dam body normally comes from the interfacial cementation of concrete. When the body of the CFRD deforms due to long-term behavior, gaps can develop between the concrete slab and the dam. Thus, to analyze the stability of a concrete slab, the interfacial behavior between the concrete slab and the dam should be considered. FLAC2D, which is a commercial finite difference method (Itasca 2008), is used for the simulation. In this study, an interface element, which is embedded in the FLAC2D, is introduced to analyze the stability of the concrete slab.

Interface elements work as shown in Fig. 6. The normal and shear stiffness can govern the behavior of contact between the concrete slab and the rock-fill and furthermore the interface element in FLAC2D can control slipping and bonding. The bond between concrete slab and transient layers, which exists even in a minute amount, has been ignored for simplicity in the conventional numerical modeling. In this study, it is assumed that the adhesion between the slab and the dam body is breakable bonding. The relative movement between the slab and the dam body will not be developed if the tensile strength of the bond is higher than the tensile stress. Although it is bonded in the initial stage, the bond can be broken when the tensile stress exceeds the bond strength due to the time-dependent settlement of the dam body. Then, the relative movement can occur.

In this study, it is endeavored to find the more accurate interface properties based on the monitoring data and to derive the tensile bond properties between concrete slab and transient layer, which enable to simulate the relative movement of concrete slab and the underneath dam body more accurately. The axial and shear behavior of the concrete slab can be obtained from the numerical analysis because the concrete slab is simulated with a beam element that is attached to the grid.

For the numerical analysis, the properties of the interface element should be derived based on reliable experimental testing. However, it is difficult to obtain the interfacial properties from experimental testing for CFRD. Alternatively, the interfacial properties of the concrete slab are

estimated based on comparison to the monitored vertical displacement obtained on the concrete slab in this study.

The cross section of the highest CFRD in South Korea is shown in Fig. 7. From the large-scale triaxial test, it was found that the rock-fill that composes the main body of the CFRD can be considered as a non-linear elastic material (Duncan and Chang 1970). The Duncan-Chang model is constructed in FLAC2D to simulate the hyperbolic stress-strain behavior under loading and unloading condition for the main body of the CFRD.

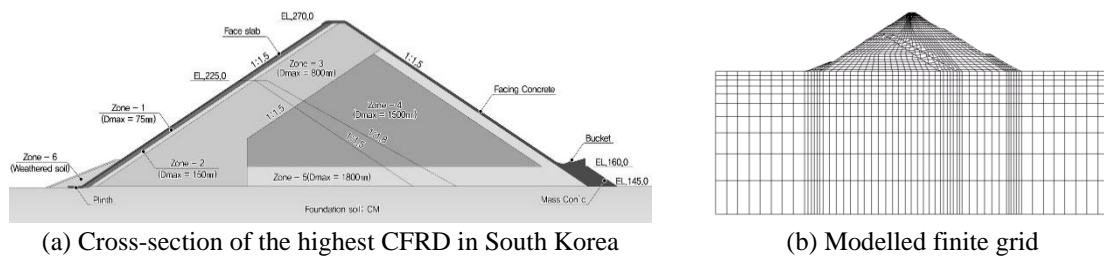


Fig. 7 Modeling of the highest CFRD in South Korea with FLAC2D

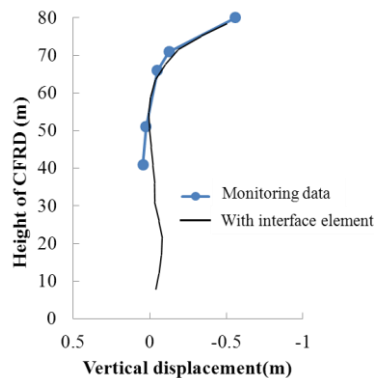


Fig. 8 Vertical displacement of the 1st concrete slab induced by the 2nd construction stage

Table 3 Material properties used in numerical analysis

Zone	1 st construction stage (t=1987)		2 nd construction stage (t=2002)		3 rd construction stage (t=2013)		At convergence (t=∞)	
	E(MPa)	K	E(MPa)	K	E(MPa)	K	E(MPa)	K
Zone 3	70.0	368	137.8	1,844	281.6	2,798	122.9	1,221
Zone 4, 5	73.2	431	133.2	1,435	272.2	2,224	118.8	970

Table 4 Estimated properties of interface element and beam element

Beam element			Interface element						
Elastic modulus (Pa)	Thickness (m)	Poisson's ratio	Normal stiffness, k_n (N/m)	Shear stiffness, k_s (N/m)	Cohesion (Pa)	Dilation angle (°)	Friction angle (°)	Tensile bond (Pa)	
2.1E9	0.8	0.2	2e7	2e7	1e4	0.0	46.0	1e5	

Zones 3, 4, and 5 take a large portion of the CFRD, as shown in Fig. 7(a). Thus, it was considered that those zones are the representative CFRD bodies. Elastic modulus (E) and modulus number (K), which were estimated using back analysis, are tabulated in Table 3. In Duncan-Chang model, K is a modulus number which governs the non-linear elastic behavior (Duncan and Chang 1970).

During the construction of the 2nd stage, from July 2003 to October 2005, the vertical displacement at the upper part of the 1st concrete slab was measured; resulting values are presented in Fig. 8. The upper part of the 1st concrete slab settled due to the 2nd construction stage; however, the lower part of concrete slab shows trivial deformation. Therefore, it can be inferred that the crack in the upper part of the 1st concrete slab was caused by large deformation in that section. A numerical model was generated to simulate the deformation behavior of the 1st concrete slab. The properties of the interface element that provide best fitting deformation curve were obtained and data are tabulated in Table 4.

Table 5 Level of reservoir for hydraulic boundary condition

Classification	Level of reservoir	Seismic load
Design level	EL. 183.0 m	-
Full level	EL. 181.0 m	-
Overflow level	EL. 273.7 m (3.7 m above the crest)	0.22 g

Table 6 Sectional forces on concrete slab after the 3rd construction stage

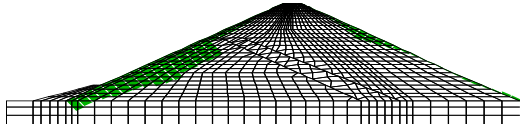
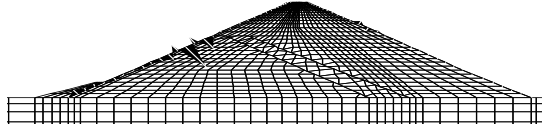
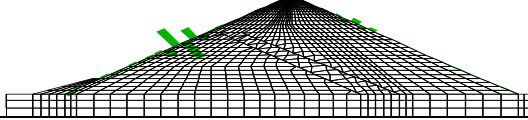
Sectional force	Diagram
Axial force	
Bending moment	
Shear force	

Table 7 Stability analysis on concrete slab after the 3rd construction stage

Classification	Slab	Bending compressive stress (MPa)			Bending tensile stress (MPa)			Shear stress (MPa)		
		Max.	Allow	Judg	Max.	Allow.	Judg.	Max.	Allow.	Judg.
Upstream	1 st	0.610	9.600	O.K.	-	0.637	O.K.	0.005	0.392	O.K.
	2 nd	0.220	9.600	O.K.	0.051	0.637	O.K.	0.002	0.392	O.K.
Downstream		0.084	9.600	O.K.	0.001	0.637	O.K.	0.001	0.392	O.K.

3.3 Stability analysis on concrete slabs during construction

The construction sequence was simulated based on the historical record and the 3rd construction plan. During the simulation of the construction sequence, static analysis was conducted. To obtain the sectional force, a Fluid-Soil-Structure interaction scheme was implemented in the numerical analysis. Thus, three different levels of the reservoir were considered in this study as presented in Table 5.

Diagrams of the sectional forces, such as the axial force, bending moment, and shear force, are summarized in Table 6; these values were determined after the construction of the concrete slab over the downstream slope (i.e., the 3rd construction stage) at full level condition. Stresses induced by sectional forces can be calculated and the stability of the concrete slab can be evaluated based on a comparison with the allowable stresses. Analysis of the stability of the concrete slab is presented in Table 7. In conclusion, stresses acting on the concrete slab do not exceed the critical stress levels.

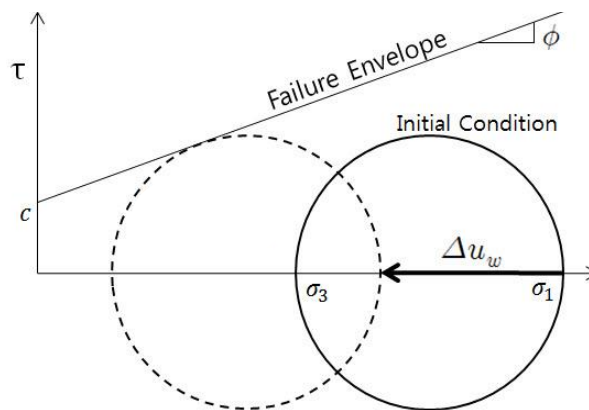
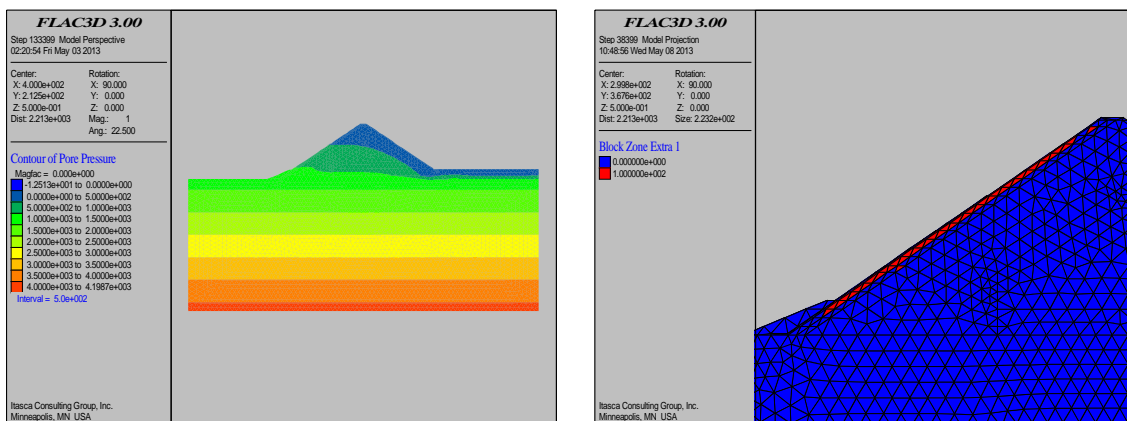


Fig. 9 Change of state of stress due to seeping through the crack in CFRD



(a) Pore-water pressure distribution in critical condition

(b) Failure behind the concrete lining under critical condition

Fig. 10 Analysis on the shear strength failure due to seeping through the crack

3.4 Stability analysis on shear strength failure during overflow

The crack of concrete slab is critical for the function of this CFRD since this CFRD should be stable during the overflow and when high pore-water pressure is acting on the concrete slab. If the concrete slab contains cracks, water will seep through the concrete slab rapidly and concrete slab will collapse. Thus, the evaluation of shear strength failure is essential for this particular CFRD.

The change of state of stress in CFRD can be simplified as follows to evaluate the shear strength failure conservatively and simply: When the radius of Mohr circle is constant and total stress maintains, Mohr circle shifts and touch the failure envelope when effective stress decreases due to increase of pore-water pressure. This process is presented in Fig. 9.

It can be assumed that the state of stress in initial condition after the 2nd construction stage. During the overflow condition when the high pore-water pressure acting on the CFRD, effective stress decreases due to the excessive pore-water pressure Δu_w . The minimum excessive pore-water pressure which can cause failure can be determined as follows

$$\Delta u_w = \sigma_3 - \frac{(\sigma_1 - \sigma_3) - 2c \cdot \tan(45 + \frac{\varphi}{2})}{\tan^2(45 + \frac{\varphi}{2}) - 1} \quad (2)$$

where σ_1 is maximum principle stress, σ_3 is minimum principle stress, c is cohesion and φ is friction angle.

FLAC3D is used to evaluate the possibility of shear strength failure for this particular CFRD in this study. The user defined code to evaluate the failure is newly developed and presented in the Mathgram 2. When any zone satisfies the failure condition, it is reported to the memory and it can be accessed anytime for post-processing.

It is assumed that seepage water can pass through the crack in concrete lining and static pore-water pressure is going to fully activated in CFRD body as it is presented in Fig. 10(a). From Fig. 10(b), it can be found that the Zone 1 behind the concrete face satisfies the shear strength failure condition under the overflow condition (i.e., water table is 3.77 m higher than crest). Thus, it can be concluded that failure will be occurred along the surface of CFRD due to the seeping through the crack. But it is not going to affect on the whole CFRD stability since the range of fractured zone is limited.

4. Conclusions

Raising the height of the highest CFRD in South Korea caused the significant deformation of dam body and upstream concrete slab. It is obvious that this CFRD is affected by subsequent construction process as well as creep behavior. However, the study on the time-dependent behavior of dam body and evaluation of the stability of concrete slabs has been insufficient so far.

The Kelvin model, which can present hyperbolic time-dependent behavior of rock-fill, was used and model parameters were estimated from the data measured in the field. Prediction of long-term behavior of the highest CFRD in South Korea is performed based on the back analysis. It takes around 20 years to reach 80% of final settlement.

Furthermore, a numerical study was conducted to estimate the stability of the concrete slab of the highest CFRD in South Korea. Especially, an interface element was introduced to simulate the contact behavior between the concrete slab and the rock-fill. Proper interfacial properties of concrete slabs are estimated based on the vertical displacement history obtained on the concrete slabs. From the analysis considering the interface between concrete slab and dam body, the

reliable inference for the cause of crack in the upper part of concrete slab becomes available.

Possibility of shear strength failure under the critical condition is also investigated based on the simplified model. It is found that failure can occur at the slope of CFRD due to the seeping through the crack on the concrete slab. However, the range of failure is limited to the shallow Zone 1.

The quality of numerical analysis result is dependent on the reliability of model and its parameters. Duncan-Chang parameters can be obtained from large-triaxial tests to predict the behavior of CFRD. However, the time-dependent creep behavior of rock-fill which governs the most significant deformation behavior of CFRD is difficult to obtain and simulate. Thus, it would be the best to obtain the settlement data right after the construction and use it for prediction of long-term behavior of CFRD. Continuous long-term monitoring and regular maintenance also should be carried out to assure the quality of the high CFRD.

Acknowledgments

This research was supported by a grant (13SCIP-B066321-01) from the Construction Technology Research Program funded by the Ministry of Land, Infrastructure, and Transport of the Korean government. Also, this work was supported by the National Research Foundation of Korea (NRF) grant funded by the Korea government (MSIT) (No. 2017R1A5A1014883).

References

- Cooke, J.B. and Sherard, J.L. (1987), "Concrete-face rockfill dam: II, design", *J. Geotech. Eng.*, **113**(10), 1113-1132.
- Das, B.M. (1997), *Advanced Soil Mechanics*, Taylor and Francis, London, U.K.
- DiMaggio, F.L. and Sandler, I.S. (1971), "Material model for granular soils", *J. Eng. Mech. Div.*, **97**(3), 935-950.
- Duncan, J.M. and Chang, C.Y. (1970), "Nonlinear analysis of stress and strain in soils", *J. Soil Mech. Found. Div.*, **96**(5), 1629-1653.
- Itasca (2005), *FLAC 3D: Fast Lagrangian Analysis of Continua in 3 Dimensions*, Version 3.0, User Manual, Itasca Consulting Group, Inc., Minneapolis, Minnesota, U.S.A.
- Itasca (2008), *FLAC 3D: Fast Lagrangian Analysis of Continua in 2 Dimensions*, Version 6.0, User Manual, Itasca Consulting Group, Inc., Minneapolis, Minnesota, U.S.A.
- Lee, H.M., Lim, H.D., Cho, G.C. and Song, K.I. (2013), "The stability evaluation of concrete face rockfill dam(CFRD) using settlement measured at the dam crest and Kelvin model", *J. Kor. Geo-Environ. Soc.*, **14**(11), 33-46.
- Ministry of Land, Transport and Maritime Affairs of Korea (2011), *Dam Design Guidelines*, Sejong, Korea.
- Prevost, J.H. and Keane, C.M. (1990), "Shear stress-strain curve generation from simple material parameters", *J. Geotech. Eng.*, **116**(8), 1255-1263.
- Shin, D.H. (2003), "Experimental study on deformation properties of bedding zone materials bearing the concrete face slab of CFRD", *Proceedings of the Annual Conference of Korean Society of Civil Engineers*, Daegu, Korea, October.
- Shin, D.H., Cho, S.E., Jeon, J.S. and Lee, J.W. (2007), "Deformation behavior of existing concrete-faced rockfill dam due to raising", *J. Kor. Geo-Environ. Soc.*, **8**(6), 77-83.
- Yoon, J.S. and Song, K.I. (2016), *Tunnel Deformation Mechanism*, CIR Press, Korea.

Appendix

Mathgram 1 Least square regression to obtain the Kelvin model parameters for 1st stage

$$\begin{aligned}
 &N := 11 \quad t_l := 0..11 \quad k := 0..N-1 \\
 &d_{ul} = \frac{\sigma \cdot (1 + 2K_0)}{9K} + \frac{\sigma \cdot (1 - K_0)}{3G} \left[1 - e^{-\frac{(G \cdot t_l)}{\eta}} \right] \\
 &d(K, G, \eta, t_l) := \left[\frac{\sigma \cdot (1 + 2K_0)}{9K} + \frac{\sigma \cdot (1 - K_0)}{3G} \left[1 - e^{-\frac{(G \cdot t_l)}{\eta}} \right] \right] \\
 &sse(K, G, \eta) := \sum_{k=0}^{N-1} \left(\text{Monitored}_k - d(K, G, \eta, t_{l_k}) \right)^2 \\
 \\
 &\text{Initial guess: } \underline{K} := 52920000 \quad \underline{G} := 14000 \quad \underline{\eta} := 55000000 \quad < \text{Input} > \\
 &\text{Given } sse(K, G, \eta) = 0 \quad K > 0 \quad G > 2000 \quad \eta > 0 \\
 \\
 &\begin{pmatrix} \underline{K} \\ \underline{G} \\ \underline{\eta} \end{pmatrix} := \text{Minerr}(K, G, \eta) \quad sse(K, G, \eta) = 5.138 \times 10^{-8} \\
 &\underline{K} = 5.292 \times 10^7 \quad \underline{G} = 1.4 \times 10^4 \quad \underline{\eta} = 5.5 \times 10^7 \\
 \\
 &d_f := \left[\frac{\sigma \cdot (1 + 2K_0)}{9K} + \frac{\sigma \cdot (1 - K_0)}{3G} \left[1 - e^{-\frac{(G \cdot t)}{\eta}} \right] \right]
 \end{aligned}$$

Mathgram 2 User defined code to evaluate the shear strength failure

```

def Shear_Strength_Failure
  pnt = zone_head
  loop while pnt # null
    if z_ycen(pnt) > 300
      de_uw_up = (z_sig1(pnt) - z_sig3(pnt)) - 2 * z_prop(pnt, 'cohesion') * tan((45 + z_prop(pnt, 'friction')/2) * 3.14/180)
      de_uw_down = (tan((45 + z_prop(pnt, 'friction')/2) * 3.14/180)) ^ 2 - 1
      de_uw = abs(z_sig3(pnt)) - abs(de_uw_up / de_uw_down)
      if z_pp(pnt) > abs(de_uw)
        z_extra(pnt, 1) = 100
      else
        z_extra(pnt, 1) = 0
      end_if
    end_if
    pnt = z_next(pnt)
  end_loop
end

```